

Crystal facets effect of tin dioxide nanocrystals on photocatalytic degradation and photo-assisted gas sensing properties

Yan Liang,^a Zhongke Xiang,^a Xiaojian Zhao,^a Feifei Xiang,^a Peipei Yan,^a Ting Yu,^b Xin Li,^b and Yong Yang^{*b}

Experimental

Materials preparation

SnO₂ nanocrystals with different crystal facets exposing were prepared by a simple hydrothermal method similarly to the previous report [1]. SnCl₄ • 5H₂O was used as Sn source. Polyvinylpyrrolidone (PVP) and HCl were used as morphology controlling agent. Typically, octahedral SnO₂ with dominated {221} crystal facets (denoted as SnO₂-Octa) was obtained as follows. 0.7 g SnCl₄ • 5H₂O, 0.63 g PVP and 1.6 mL HCl were added into the mixed solution of 12 mL of deionized water and 12 mL of ethanol under vigorous stirring. The mixture was reacted in a 50 mL Teflon-lined stainless steel autoclave. The reaction temperature was set at 200 °C and the reaction time was 12 h. After reaction, the product was thoroughly cleaned with deionized water and ethanol, and then calcined in air at 400 °C for 2 h to remove surface adsorbed impurities. Elongated octahedral SnO₂ with coexisted {221} crystal facets and {110} crystal facets (denoted as SnO₂-Elongated octa) and lance shaped SnO₂ with dominated {110} crystal facets (denoted as SnO₂-Lance shaped) were prepared similar to the above method except that 1.2 mL and 2.0 mL of HCl were used instead of 1.6 mL HCl, respectively.

Materials characterization

X-Ray diffraction patterns (XRD) measurement were conducted on a Malvern Panalytical X-ray diffractometer. Scanning electron microscopy (SEM) and transmission electron microscopy (TEM) images were recorded by a ZEISS EVO microscope and JEM-2100 microscope, respectively. Nitrogen adsorption-desorption measurement was conducted by a BET analyzer (Micro for TriStar II Plus 2.02). X-ray photoelectron spectroscopy (XPS) analysis was conducted on a Thermo Fisher Scientific spectrometer (Escalab 250Xi) which was employed with Al K α radiation. UV-Vis absorption spectra were obtained using a U-3310 UV-Vis spectrometer by Hitachi.

Photoelectrochemical measurement

The transient photocurrent were tested using electrochemical work station (CHI 760D) in a standard three electrode system with a working electrode, a Pt counter electrode, and a Ag/AgCl reference electrode. The working electrode was prepared by drop-casting 0.4 mL of the SnO₂ powders onto an indium tin oxide (ITO) glass, the SnO₂ powders were dispersed in aqueous solution (6 mg/mL) previously. The working electrode was dried at 60 °C in vacuum. The electrolyte was 0.5 M sodium sulphite aqueous solution. A 500 W Xe lamp was employed for light irradiation.

Measurement of photocatalytic performance

Photocatalytic activity in the degradation of trace water pollutants were tested using high pressure mercury lamp as light source. The radiation of high-pressure mercury lamp used in the photocatalytic reaction is in the ultraviolet region, and the wavelength of main peak is 365 nm. The power of high-pressure mercury lamp is 1000 W, and the radiant flux entering the reactor is about $10.22 \mu\text{W}/\text{cm}^2$. Two typical organic dyes methyl orange (MO) and methylene blue (MB) were selected as target water pollutants. 20 mg SnO_2 powder was added into 40 mL MO and MB solution with a concentration of 20 mg/L, 0.3 mL H_2O_2 was used as electron trapping agent. Before the light open, the suspensions were ultrasonicated and magnetically stirred in dark condition for 30 min. The photocatalytic degradation was conducted in a commercial photochemical reaction instrument (Shanghai Yuming Instrument Co. Ltd.). After a given time interval, 2 mL analysis sample was taken out, and then centrifuged to isolate the liquid sample from the solid photocatalyst powder for analysis. The UV-Vis absorption spectra of the pollutants solutions were recorded using a Hitachi U-3310 UV-Vis spectrometer. The concentration change of MO and MB were determined by the absorption peak at 464 and 664 nm, respectively.

Measurement of gas sensing performance

The fabrication of gas sensor was similar to our previous report [21]. First, certain amount of SnO_2 powder was dispersed in ethanol through intense ultrasonic treatment to obtain a paste. Then the paste was dropped onto an commercial alumina flat which had been coated with Pt-interdigitated electrodes (produced by Huachuang Ruike Science and Technology Co. Ltd.). After the alumina flat was dried, it was calcinated at $400 \text{ }^\circ\text{C}$ for 2 h to form a gas sensor. The gas sensing properties was tested on a

commercially static testing device (produced by Huachuang Ruike Science and Technology Co. Ltd.). During the tests, LED UV light was used to illuminate the sensor, target gases were injected into the test chamber, and then the chamber was lifted to introduce ambient air. The wavelength of main peak of the LED UV light used in gas sensing experiments is 365 nm, and the radiant flux entering the surface of the sensor is about 1.353 $\mu\text{W}/\text{cm}^2$. The operating temperature of the sensor was set to room temperature (25 °C).

Method of calculation

To explore the related mechanism, the density functional theory (DFT) calculation was conducted with the Vienna Ab-Initio Simulation Package [2]. The electron-ion interaction was described by projector augmented-wave (PAW) pseudopotentials. For the exchange and correlation functionals, the Perdew-Burke-Ernzerhof (PBE) version of the generalized gradient approximation (GGA) exchange-correlation was applied [3,4]. During the calculation, the kinetic energy cutoff of 450 eV was used for the wave functions expansion. Brillouin zone integration on the grid with $3\times 3\times 1$ for geometry optimization and $5\times 5\times 1$ k-grid mesh for calculation of density of states. The energy and force converged to 1.0×10^{-5} eV atom⁻¹ and 0.03 eV·Å⁻¹ to achieve high accuracy. Vacuum layer thickness of 25 Å was applied to avoid virtual interaction and obtain more accurate results. The structures of SnO₂ (110) facet and SnO₂ (221) facet were used to uncover the electronic properties. And, the corrected adsorption energy of NH₃ on the SnO₂ surface (ΔE_{ads}) is defined as:

$$\Delta E_{ads} = E_{NH_3 + SnO_2} - E_{SnO_2} - E_{NH_3}$$

Where $E_{NH_3 + SnO_2}$ is the total energy of SnO₂ facets adsorbed with NH₃, E_{SnO_2} is the total energy of SnO₂ facets, and E_{NH_3} is the total energy of NH₃ gas.

Reference:

1. X. G. Han, M. S. Jin, S. F. Xie, Q. Kuang, Z. Y. Jiang, Y. Q. Jiang, Z. X. Xie and L. S. Zheng, *Angew. Chem. Int. Edit.*, 2009, **48**, 9180-9183.
2. G. Kresse and D. Joubert, *Phys. Rev. B*, 1999, **59**, 1758–1775.
3. J.P. Perdew, K. Burke and M. Ernzerhof, *Phys. Rev. Lett.*, 1996, **77**, 3865–3868.
4. P.E. Blöchl, *Phys. Rev. B*, 1994, **50**, 17953.

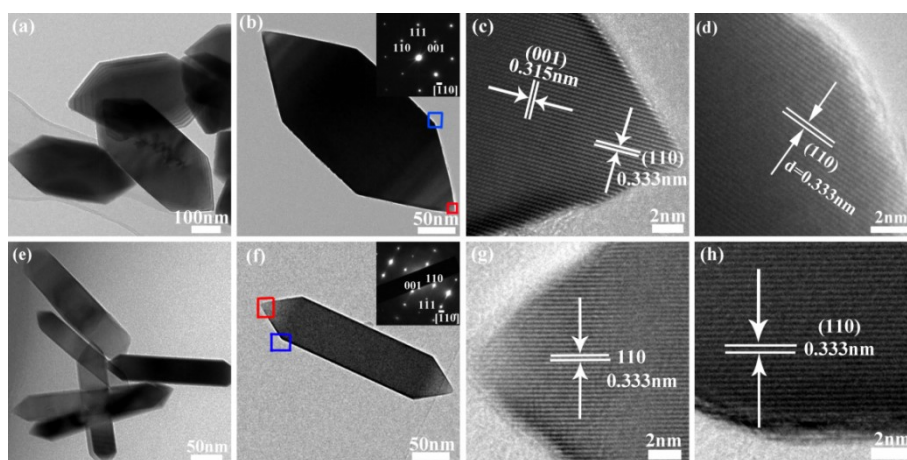


Fig. S1 (a) and (b) TEM images of SnO₂-Elongated octa, inset in (b) is the SAED image; (c) and (d) HRTEM of SnO₂-Elongated octa taken from the red area and blue area of (b), respectively; (e) and (f) TEM images of SnO₂-Lance shaped, inset in (f) is the SAED image; (g) and (h) HRTEM of SnO₂-Lance shaped taken from the red area and blue area of (f), respectively.

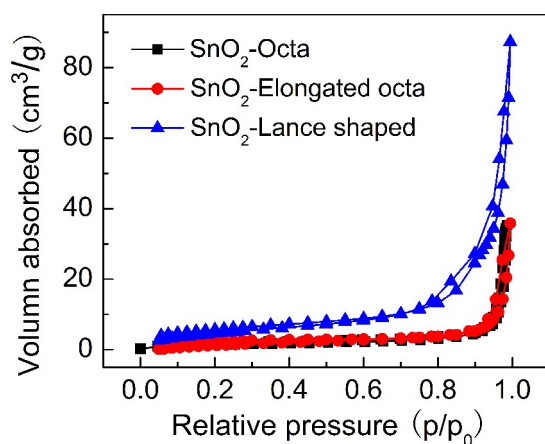


Fig. S2 Nitrogen adsorption-desorption isotherms of the different samples.

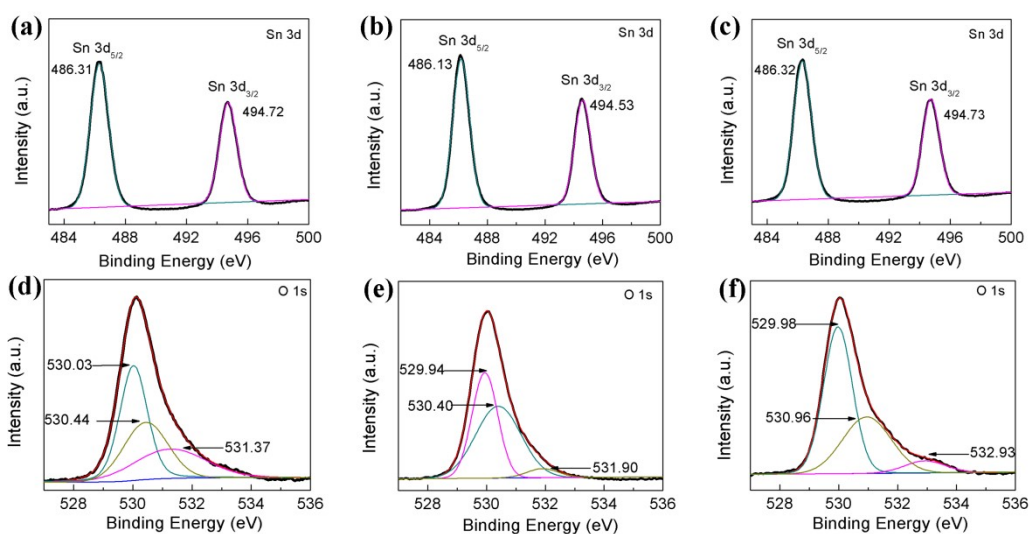


Fig. S3 High-resolution XPS spectra of the different samples: (a) and (d) SnO₂-Octa; (b) and (e) SnO₂-Elongated octa; (c) and (f) SnO₂-Lance shaped.

Table S1 Detailed XPS results of O 1s of the different samples.

Sample	lattice oxygen	oxygen vacancy	chemisorbed oxygen
SnO ₂ -Octa	43.05 %	31.22 %	25.73 %
SnO ₂ -Elongated octa	43.36 %	52.11 %	4.53 %
SnO ₂ -Lance shaped	57.42 %	36.11 %	6.47 %

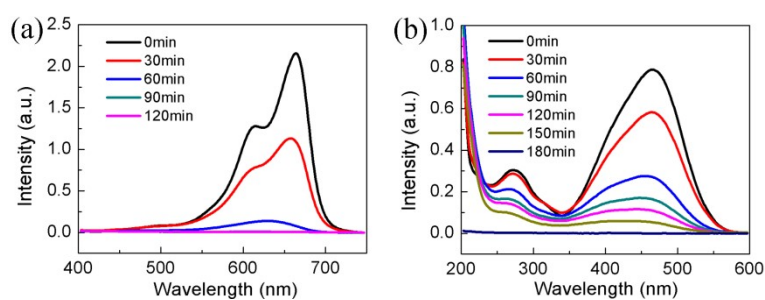


Fig. S4 Time-dependent optical absorbance spectra of (a) MB and (b) MO solution in the presence of SnO₂-Elongated octa.

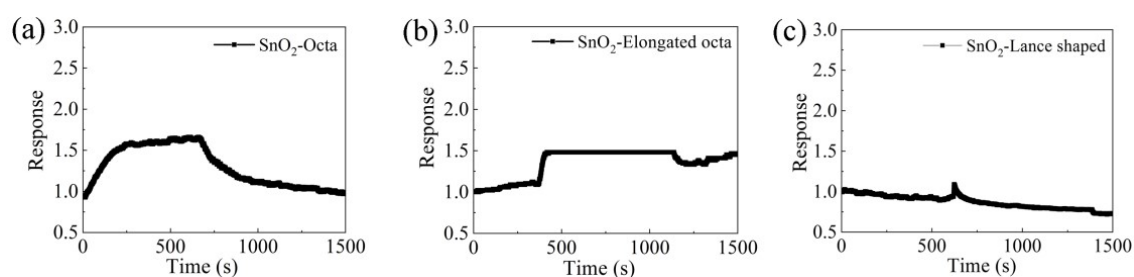


Fig. S5 Typical dynamical response/recovery transients of the different SnO₂ towards 100 ppm ammonia at room temperature without light assistance .

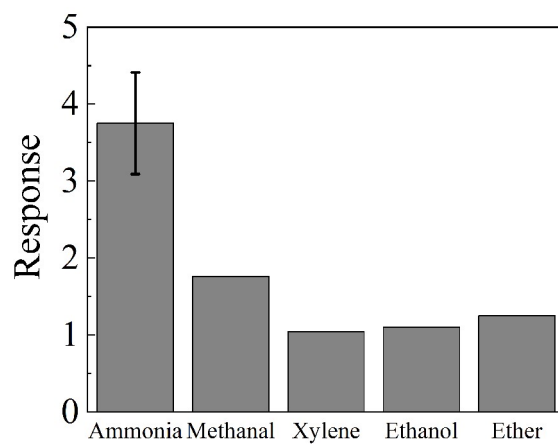


Fig. S6 Selectivity of SnO₂-Octa towards various gases.

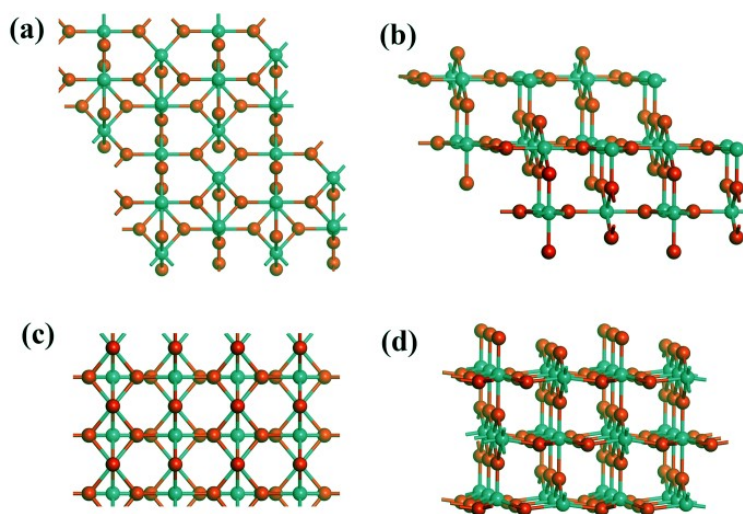


Fig. S7 (a) Top and (b) side view of the atomic configuration of SnO₂ {221} crystal facets; (c) Top and (d) side view of the atomic configuration of SnO₂ {110} crystal facets.

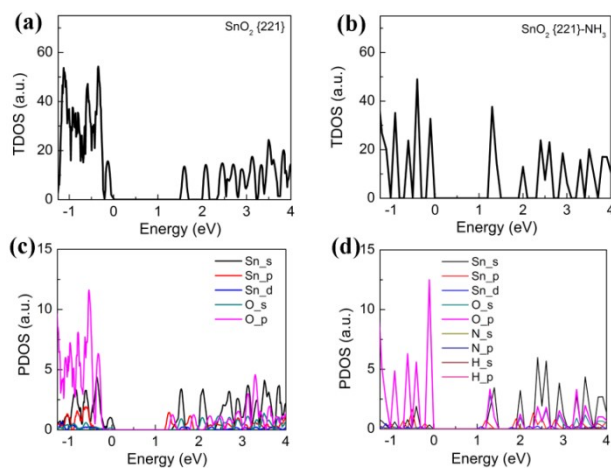


Fig. S8 The TDOS and PDOS of SnO₂ {221} facets (a) and (c) before and (b) and (d) after adsorption of ammonia gas.